Ab initio calculations of the temperature-dependent magnetostriction of Fe and A2 $Fe_{1-x}Ga_x$ within the disordered local moment picture: Supplemental material

George A. Marchant, Christopher E. Patrick, Julie B. Staunton
Department of Physics, University of Warwick, Coventry CV4 7AL, United Kingdom

December 20, 2018

1 Computational method comparisons

1.1 Torque vs. Strain: Validity of linear regime

In Fig. 1 we plot the torque T_θ ($\theta = \pi/4$) as a function of tetragonal strain ϵ_{zz} at a =5.40 a.u., where the frozen potential approximation has not been used and thus the potentials generated in Step 1. of the method in Section II.D are generated in the strained system. We see that, compared to the results shown in Fig. 1 of the main article, there is a more significant non-linear contribution when $m \sim 1$. At $m = 0.72$ we observe almost zero non-linear dependence. However, it is worth noting that using either a quadratic or linear fitting procedure (shown on the left and right of the figure respectively) leads to the same value of B_1 within 3 significant figures, so the system can still be reasonably considered within the linear regime.

1.2 Muffin-tin vs. Atomic sphere approximation

In Figure 2 we compare B_1 vs. m curves at a =5.20 and 5.40 a.u. when using muffin-tin (MT) (used in the main article) and atomic sphere approximation (ASA) potentials. All other variables in the method are consistent with the main article.

We find that the use of the ASA potentials leads to some quantitative changes to B_1 at particular temperatures, e.g. $B_1 \sim -4$ MJ/m^3 at zero temperature compared to ~ -2 MJ/m^3 when using MT at a =5.40 a.u.. It is clear however that the key features of the temperature and volume dependence are very similar between the two methods, such as the peak in B_1 of $\sim$-8 MJ/m^3 at m =0.8 when a =5.40 a.u., as well as the decrease in B_1 with increasing lattice parameter and the convergence of isovolumetric curves at high temperature.

1.3 Frozen vs. self consistent potentials

In Figure 3 we compare B_1 vs. m curves at a =5.20 and 5.40 a.u. when using frozen potentials and self consistent potentials, referring to whether the potentials generated in Step 1 of the method in Section II.D are done so in the cubic or strained system respectively. All other variables in the method are consistent with the main article.

There are certainly quantitative differences in B_1 between the frozen and self-consistent distortions at certain values of m. For example at $m = 1$ the frozen distortion gives $B_1 = -2.5$ MJ/m^3 at $a = 5.40$ a.u. while self consistent distortions give $B_1 = -1.7$ MJ/m^3. The initial decrease in B_1 between m =1 and 0.95 at a =5.40 a.u. is greater in the frozen case also, almost twice as much. However key features such as the volume dependence, the location and magnitude of the peak in B_1 (around m =0.8 and B_1 =-8 MJ/m^3) and the isovolumetric convergence at high temperature are entirely consistent. These results show that the conclusions we arrive at in this manuscript are not meaningfully affected by this choice, nor the choice of MT or ASA potentials.

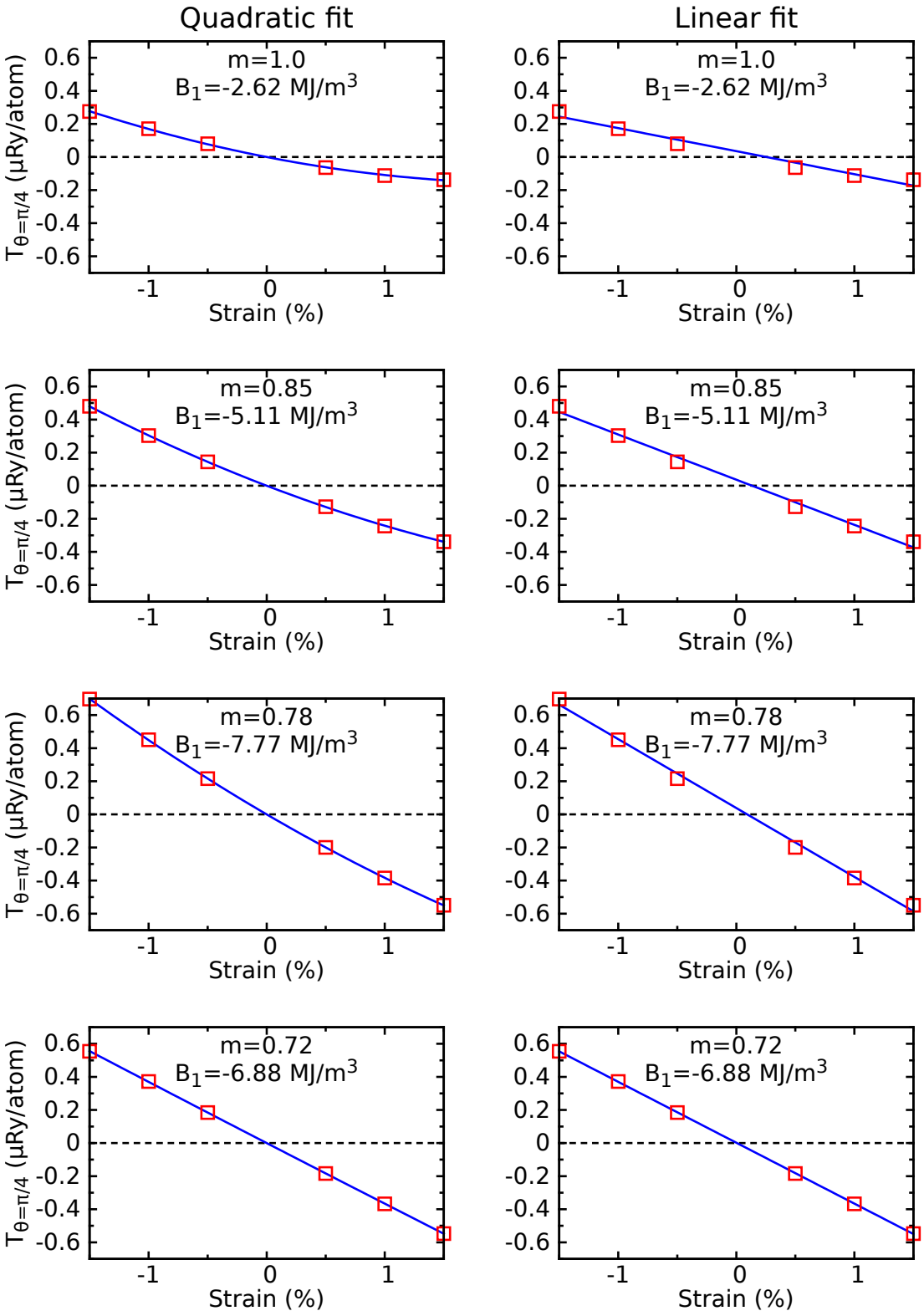

Figure 1: Torque T_θ ($\theta = \pi/4$) as a function of tetragonal strain ϵ_{zz} for different magnetic order parameters m, while using strained potentials i.e. no frozen potential approximation (FPA). Left: Data fitted with quadratic function $A + B_1 x + C x^2$, where B_1 is the magnetoelastic constant. Right: Data fitted with linear function $A + B_1 x$. Included on each graph are values for B_1 for each fitting procedure.

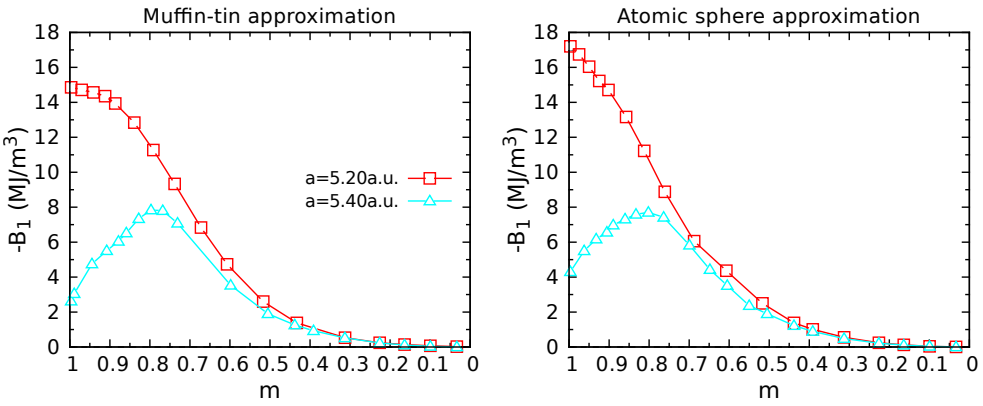

Figure 2: Magnetoelastic constant B_1 as a function of order parameter m at a =5.20 a.u. (squares, red) and a =5.40 a.u. (triangles, blue), using the muffin-tin (left) and atomic sphere (right) approximations.

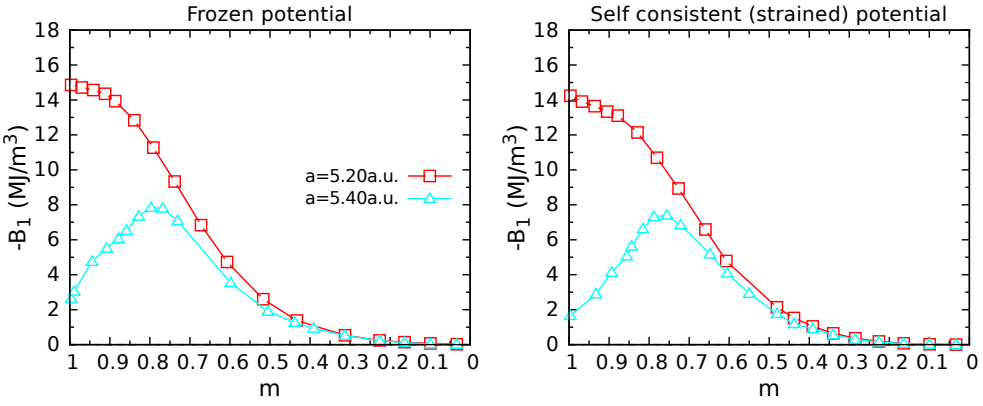

Figure 3: Magnetoelastic constant B_1 as a function of order parameter m at a =5.20 a.u. (squares, red) and a =5.40 a.u. (triangles, blue), using the frozen (left) and self-consistent i.e. strained (right) potentials.

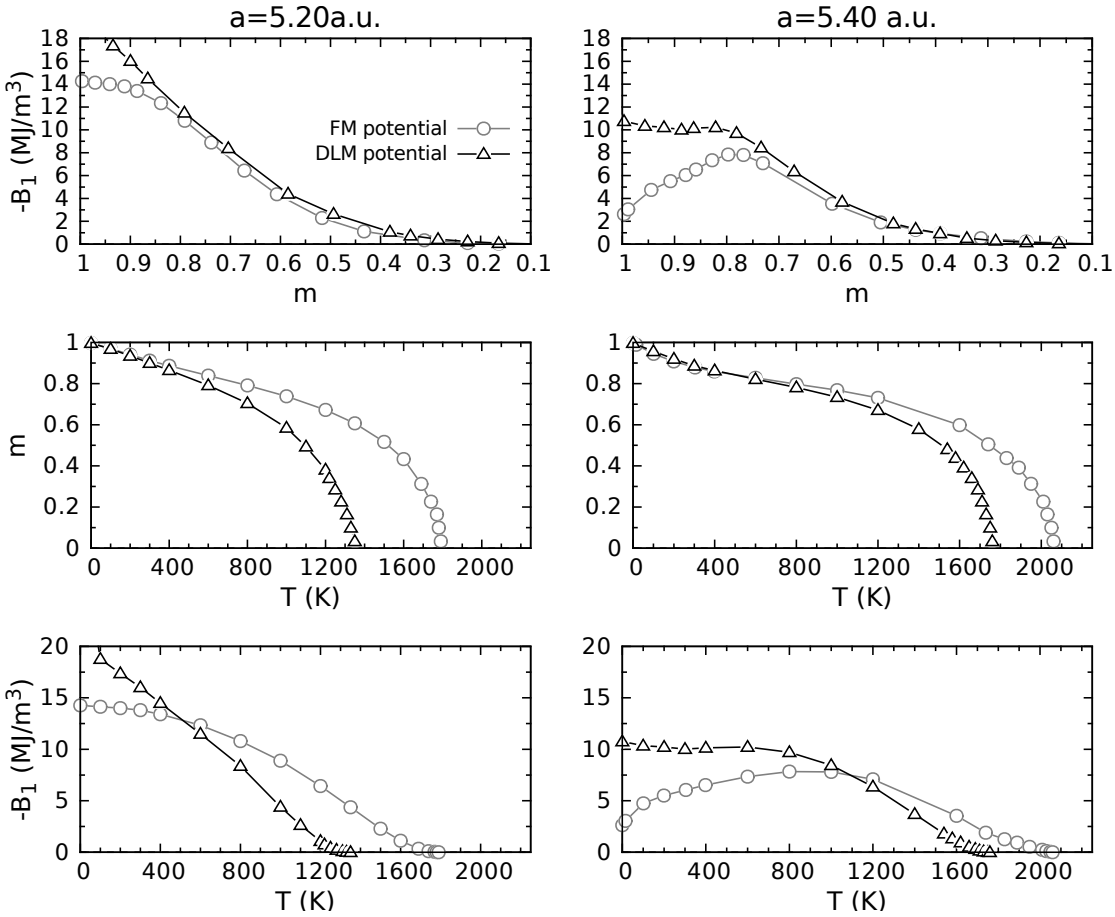

Figure 4: Top: Magnetoelastic constant B_1 as a function of order parameter m at a =5.20 a.u. (left) and a =5.40 a.u. (right), using FM potentials (circles, grey) and DLM potentials (triangles, black). Middle: Order parameter m as a function of temperature T at a =5.20 a.u. (left) and a =5.40 a.u. (right), using FM potentials (circles,grey) a and DLM potentials (triangles,black). Bottom: Magnetoelastic constant B_1 as a function of temperature T at a =5.20 a.u. (left) and a =5.40 a.u. (right), using FM potentials (circles,grey) and DLM potentials (triangles,black).

1.4 Ferromagnetic vs. paramagnetic (DLM) potentials

In Fig. 4 we compare B_1 vs. m, m vs. T and B_1 vs. T when using either DLM or FM potentials. We see that significant disparities arise between the B_1 vs. m curves when $m > 0.6$, such as the lack of a prominent peak in B_1 in the DLM case. As this is the region in which the FM potential is more physically justified, it should be considered a more reliable description of the system. We can see that the B_1 vs. m curves converge upon the same behaviour as m decreases, with significant agreement achieved around $m = 0.5$. This means that studying only the behaviour of the FM potential, at least for this particular system, is sufficient for the entire ferromagnetic range.

Also plotted in Fig. 4 is a comparison between choice of potential with regards to magnetic order as a function of temperature for a =5.20 a.u. and a =5.40 a.u. Here we see a significant difference between the choice of potential at high T and, as should be expected, we have a better estimate of T_C when using DLM potentials. Due to the good agreement between the two potentials at low T, using only the DLM potential provides a better description of the system.

Difficulty arises when considering B_1 vs. T, which does not have an obvious choice of potential for its entire ferromagnetic range. In this case a fully self-consistent approach should be employed based on the comparative energies of the two potentials, as demonstrated in Ref 24 of the main article.

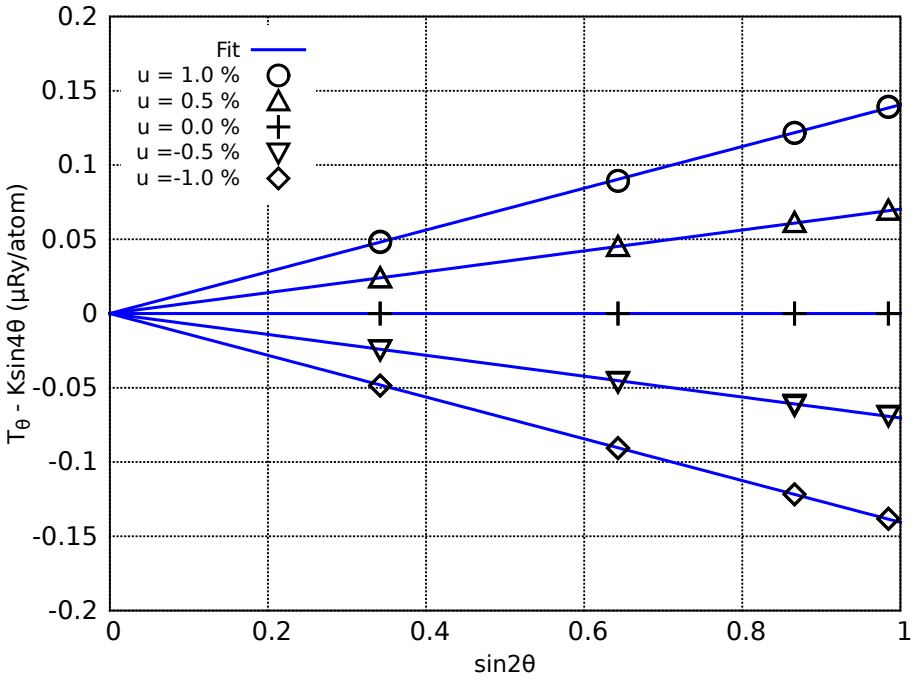

Figure 5: $T_\theta - K\sin 4\theta$ as a function of $\sin 2\theta$ with tetragonal strains of $u = 1.0$ (circles), 0.5 (up triangle), 0.0 (cross), -0.5 (down triangle), 1 % (diamond), where T_θ is magnetic torque $\partial F/\partial\theta$, θ is angle of magnetisation with respect to z axis and $K\sin 4\theta$ is the cubic anisotropy term in the model $T_\theta = K\sin 4\theta + B\sin 2\theta$, to which the data for each strain has been fit (K determined only at u =0.0%). The calculated fitting parameters are $B_{+1.0\%} = 0.140(1)$ μRy/atom, $B_{+0.5\%} = 0.0704(1)$ μRy/atom, $B_{-0.5\%} = -0.0703(3)$ μRy/atom, $B_{-1.0\%} = -0.141(1)\mu$Ry/atom, where the number in parantheses is the standard error on the last significant figure.

1.5 Torque as a function of magnetization direction

In order to determine the validity of the model

$$T_\theta = K\sin 4\theta + Bu\sin 2\theta, \tag{1}$$

where $K\sin 2\theta$ is the cubic anisotropy energy and $Bu\sin 2\theta$ is the linear magnetoelastic energy (u is the tetragonal strain in z and θ is angle of magnetisation with respect to z axis), we plot $T_\theta - K\sin 2\theta$ as a function of $\sin 2\theta$ in Fig. 5. The clear linearity in the top plot shows that the model is accurate and that no higher order terms of any significance exist.